Monthly Notices
of the
ROYAL ASTRONOMICAL SOCIETY

MNRAS **469,** 2380–2386 (2017)
Advance Access publication 2017 April 26

doi:10.1093/mnras/stx996

Derivation of capture probabilities for the corotation eccentric mean motion resonances

Maryame El Moutamid,[1,2]★ Bruno Sicardy[3] and Stéfan Renner[4]

[1]*Department of Astronomy, Cornell Center for Astrophysics and Planetary Science, Cornell University, Ithaca, NY 14853, USA*
[2]*Carl Sagan Institute, Cornell University, Ithaca, NY 14853, USA*
[3]*LESIA, Observatoire de Paris, CNRS UMR 8109, Université Pierre et Marie Curie, Université Paris-Diderot, 5 place Jules Janssen, F-92195 Meudon Cedex, France*
[4]*IMCCE, Observatoire de Paris, CNRS UMR 8028, Université Lille 1, Observatoire de Lille 1 impasse de l'Observatoire, F-59000 Lille, France*

Accepted 2017 April 24. Received 2017 April 13; in original form 2016 September 5

ABSTRACT

We study in this paper the capture of a massless particle into an isolated, first-order corotation eccentric resonance (CER), in the framework of the planar, eccentric and restricted three-body problem near a $m + 1$: m mean motion commensurability (m integer). While capture into Lindblad eccentric resonances (where the perturber's orbit is circular) has been investigated years ago, capture into CER (where the perturber's orbit is elliptic) has not yet been investigated in detail. Here, we derive the generic equations of motion near a CER in the general case where both the perturber and the test particle migrate. We derive the probability of capture in that context, and we examine more closely two particular cases: (i) if only the perturber is migrating, capture is possible only if the migration is outward from the primary. Notably, the probability of capture is independent of the way the perturber migrates outward; (ii) if only the test particle is migrating, then capture is possible only if the algebraic value of its migration rate is a decreasing function of orbital radius. In this case, the probability of capture is proportional to the radial gradient of migration. These results differ from the capture into Lindblad eccentric resonance (LER), where it is necessary that the orbits of the perturber and the test particle converge for capture to be possible.

Key words: methods: analytical – celestial mechanics – planets and satellites: dynamical evolution and stability.

1 INTRODUCTION

Orbital capture into mean motion resonance (MMR) is the key towards understanding the orbital evolution of satellites, rings and planets. The special case of the Lindblad eccentric resonance (LER) has been investigated by many authors in the context of the planar, circular and restricted three-body problem (RTBP), see the two references given below.

In this case, a secondary object orbiting a massive primary body perturbs a massless particle, so that the critical angle $\phi_L = (m + 1)\lambda_s - m\lambda_p - \varpi_p$ librates, where m is an integer, λ_s and λ_p are the longitudes of the secondary and the test particle, respectively, and ϖ_p is the longitude of pericentre of the test particle. In a general context, Henrard (1982) estimated the probability of capture into a first-order LER, while Borderies & Goldreich (1984) extended this work and derived capture probabilities into $m + 1$:m and $m + 2$: m (second order) LERs.

If the orbit of the secondary is *eccentric*, a corotation eccentric resonance (CER) appears close to and associated with each LER. It is dynamically described by the critical angle $\phi_c = (m + 1)\lambda_s - m\lambda_p - \varpi_s$, where ϖ_s is the longitude of the secondary pericentre. The physical effects of LERs and CERs are not the same: the CER mainly affects the semimajor axis of the test particle and keeps its orbital eccentricity almost constant, forcing the particle to librate inside the so-called corotation sites like a simple pendulum. In contrast, the LER acts on its eccentricity but keeps the semimajor axis almost constant (El Moutamid, Sicardy & Renner 2014).

In this work, we derive the probability of capturing a test particle into an isolated CER, as both the secondary and the particle suffer orbital migration that secularly changes their semimajor axes. This is a novel calculation that complements what has been done before in the case of LERs. The term 'isolated' means here that the CER and LER are sufficiently pulled apart so that their coupling is negligible. Eventually, the goal is to extend the study of captures into MMR to more realistic cases where both the CER and LER act in concert on the particle, but this will not be considered here.

★ E-mail: maryame@astro.cornell.edu

This work can be applied to many situations including the context of planetary rings and satellites. In the Saturnian system for example, the satellites Aegaeon, Anthe and Methone are, respectively, captured into 7:6, 10:11 and 14:15 CERs with Mimas (Cooper et al. 2008; Hedman et al. 2009, 2010; El Moutamid et al. 2014). Atlas is in a 54:53 CER with Prometheus (Renner et al. 2016). In the case of the Neptunian system, Adams ring arcs may be dynamically confined by the satellite Galatea via corotation resonances (Goldreich, Tremaine & Borderies 1986; Porco 1991; Nicholson, Mosqueira & Matthews 1995; Foryta & Sicardy 1996; Sicardy et al. 1999; Namouni & Porco 2002; Renner et al. 2014).

We note here that the capture of a particle into a CER bears some resemblance with the capture of a rotating body into spin–orbit resonance (Goldreich & Peale 1966). In both cases, a slow effect (orbital migration in our case, tidal friction for the spin–orbit resonances) drives a pendulum-like system into a librating state, possibly capturing it permanently into that state. This will be commented later.

The paper is structured as follows. In Section 2, we describe the dynamical structure of our problem based on the so-called CorALin model and include the migration parameters. In Section 3, we study the particle and the secondary migration terms involved in the derivation of the probability of capture. The latter is derived in Section 4 and confirmed in Section 5 by full numerical simulations. In Section 6, we discuss the similarity of our problem with the capture in spin–orbit resonance and finally, summary and conclusions are given in Section 7.

2 DYNAMICAL STRUCTURE OF THE PROBLEM

We consider the restricted, planar (but *not* circular) three–body problem, in which a test particle orbits around a central mass M_c, near a first order MMR $m+1$:m[1] with a perturbing secondary of mass m_s and an orbital eccentricity e_s. The various quantities and notations used hereafter are defined in Table 1.

Near the resonance, the equations of motion reduce to a two degree of freedom system associated with the two critical angles ϕ_c and ϕ_L. The subscripts c and L refer to eccentric corotation and Lindblad resonances (CER and LER, respectively). Details are given by El Moutamid et al. (2014), who encapsulated the equations of motion of the test particle in the so-called CorALin model,[2]

$$\begin{cases} \mathrm{d}J_c/\mathrm{d}\tau = -\epsilon_c \sin(\phi_c) \\ \mathrm{d}\phi_c/\mathrm{d}\tau = \chi \\ \mathrm{d}h/\mathrm{d}\tau = -(\chi + D)k \\ \mathrm{d}k/\mathrm{d}\tau = +(\chi + D)h + \epsilon_L, \end{cases} \tag{1}$$

where $\tau = n_0 t$ is a dimensionless time-scale and n_0 is the mean motion at exact corotation.[3] The strengths of the corotation and Lindblad resonances are quantified by the parameters ϵ_c and ϵ_L, respectively (see Table 1).

The CorALin model portrays two coupled resonances: a CER described by a simple pendulum system [first two equations in equations (1)], coupled to the LER given by the last two equations [the so-called second fundamental model for resonance (Henrard 1982; Henrard & Lemaitre 1983)]. The dimensionless parameter D measures the distance (*in frequency*) between the two resonances and acts as a coupling parameter between the two. For large Ds, the resonances decouple and for $\chi = 0$, only the simple-pendulum motion is relevant, while the particle eccentricity $e_p \propto \sqrt{(h^2+k^2)}$ remains constant.

Stable oscillations of ϕ_c occur around $\phi_c = 0$ (respectively $\phi_c = \pi$) for ϵ_c positive (respectively negative), with periods $\sim 2\pi/\sqrt{|\epsilon_c|}$ in the CorALin time unit, or $\sim 2\pi/(n_0\sqrt{|\epsilon_c|})$ in the usual time unit. Moreover, the full width (in units of χ) of the corotation site is $W = 4\sqrt{|\epsilon_c|}$, or

$$W_{\mathrm{CER}} = \frac{8a_0\sqrt{|\epsilon_c|}}{3|m|} \tag{2}$$

in physical distance units.[4]

The decoupling between the CER and LER occurs for

$$D_{\mathrm{CL}} >\sim W_{\mathrm{CER}}, \tag{3}$$

where D_{CL} is the radial splitting between the resonances and given by

$$D_{\mathrm{CL}} = \frac{2a_0}{3m}\left(\frac{\dot{\varpi}_s - \dot{\varpi}_p}{n_0}\right). \tag{4}$$

The condition (3) is fulfilled in the right-hand panels of Fig. 1. This figure shows that for intermediate values of D_{CL}, the CER and LER are superimposed and strongly coupled, leading to chaotic behaviour. However, the system is again an integrable one as $D_{\mathrm{CL}} = 0$.

We will restrict our study to the case of large D_{CL}s only (equation 3), and consider the effect of orbital migrations of *both* the secondary and the test particle. This causes a secular variation

Table 1. Variables, parameters and notations used in the text.

Quantities	Definitions
ϕ_c	$(m+1)\lambda_s - m\lambda_p - \varpi_s$
ϕ_L	$(m+1)\lambda_s - m\lambda_p - \varpi_p$
h	$\sqrt{3} \mid m \mid e_p \cos(\phi_L)$
k	$\sqrt{3} \mid m \mid e_p \sin(\phi_L)$
χ	$3m\Delta a/2a_0 = 3m(a_p - a_0)/2a_0$
J_c	$\chi + (h^2+k^2)/2$
ϵ_L	$\sqrt{3} \mid m \mid (m_s/M_c)(a_0/a_s)A_m$
ϵ_c	$3m^2(m_s/M_c)(a_0/a_s)A'_m e_s$
D	$(\dot{\varpi}_s - \dot{\varpi}_p)/n_0$

Notes. λ, ϖ, a, e denote the mean longitude, longitude of periapse, semimajor axis and eccentricity, respectively, and $\dot{\varpi}$ denotes the secular apsidal precession rate (e.g. forced by the oblateness of the central body or other perturbing secondaries). Subscripts s and p refer to the secondary and test particle, respectively. Subscript 0 is used for quantities estimated at the exact corotation radius, a_0. The quantities A_m and A'_m are combinations of Laplace coefficients with $A_m \sim -A'_m \sim 0.8m$ for large $|m|$s. The quantities $\dot{\varpi}$ and $\dot{\varpi}_s$ are the rate of precession of the orbits of the test particle and the secondary, respectively.

[1] The case m positive (respectively negative) implies that the particle orbits inside (respectively outside) the secondary orbit.

[2] The presentation of the CorAL in model here is slightly different from the one given in El Moutamid et al. (2014). The main differences are the sign of ϕ_L and the presence of the parameter ϵ_c, which provides a better understanding of the physical effect of a corotation resonance.

[3] Note that the time-scale used later in this paper is the usual time t, and not τ.

[4] Note that m and ϵ_c have opposite signs.

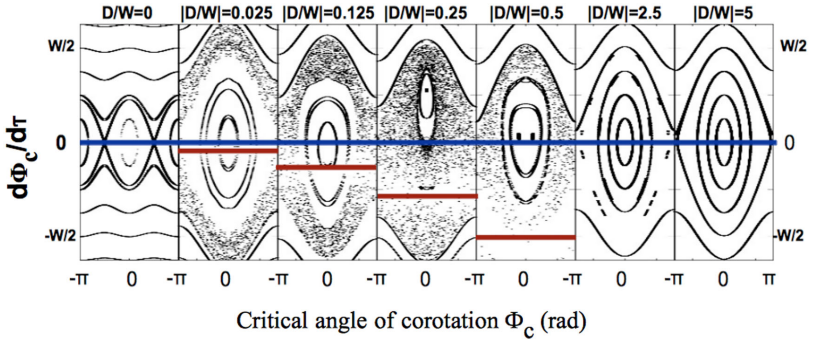

Figure 1. Poincaré surfaces of section of system (1) using $\epsilon_L = -0.1$, $\epsilon_c = 1$ and $m = 1$ (resonance 2:1) for seven different values of D. Each section is obtained when $k = 0$ and $\dot{k} > 0$ for 15 different initial conditions with the same value of energy. Note that $\tau = n_0 t$ is a dimensionless time-scale (more details are given in the text). For $D = 0$ and large Ds, the trajectories are regular, while chaos is dominant for intermediate cases, see more details in El Moutamid et al. 2014. The blue lines represent the position of the centre of CER, while the red lines represent the position of the centre of the LER.

of χ (beyond the effect of the CER) since both a_p and a_0 slowly change.

At this point, it is important to note that χ (a local form of the particle semimajor axis, see Table 1) is *not* the appropriate action variable to use together with the angle ϕ_c. Instead, an angular momentum-type quantity should be used to avoid cumbersome additional terms in the equations of motion in the presence of migration and permit the use of adiabatic invariance arguments. Here, we choose the variable $J_\phi = 3m(J_p - J_0)$ as the conjugate of ϕ_c, where J_p is the specific angular momentum of the particle and $J_0 = \sqrt{GM_c a_0}$ is the specific angular momentum at radius a_0 (G being the gravitational constant). As the CER has a very small effect on eccentricity in the absence of LER (El Moutamid et al. 2014), we can assume here that the particle has a circular orbit, then $J_\phi = \chi J_0$ is proportional to χ.

In the absence of migration, the Hamiltonian that locally describes the simple-pendulum motion near the CER reads

$$\mathcal{H}_0 = \left(\frac{GM_c}{J_0}\right)^2 \left[\frac{1}{2}\left(\frac{J_\phi}{J_0}\right)^2 - \epsilon_c \cos(\phi_c)\right], \tag{5}$$

with the correct dimension of a specific energy [see Sicardy & Dubois (2003) for details on the method].

We now define ϵ_s (respectively ϵ_p) as the dimensionless secular migration rates of the secondary (respectively test particle):[5]

$$\epsilon_s = \frac{1}{n_0 a_0}\cdot\frac{da_0}{dt} = \frac{2}{n_0 J_0}\left(\frac{dJ_0}{dt}\right)_{mig}$$
$$\epsilon_p = \frac{1}{n_0 a_0}\cdot\frac{da_p}{dt} = \frac{2}{n_0 J_0}\left(\frac{dJ_p}{dt}\right)_{mig}, \tag{6}$$

where the 'mig' index means the secular effect of the migration on the variation of J_0 and J_ϕ.

Those migration rates introduce additional terms $\dot{J}_\phi = (3m/2)n_0 J_0(\epsilon_p - \epsilon_s)$ in the equations of motion.[6] They can be incorporated in $\mathcal{H}_0$ to form a new Hamiltonian:

$$\mathcal{H} = \left(\frac{GM_c}{J_0}\right)^2 \left[\frac{1}{2}\left(\frac{J_\phi}{J_0}\right)^2 - \epsilon_c \cos(\phi_c) + \frac{3}{2}m\epsilon_{mig}\phi_c\right], \tag{7}$$

[5] Strictly speaking, ϵ_s actually measures the migration rate of the resonance radius a_0, related to the secondary migration rate by $da_0/dt = [m/(m+1)]^{2/3}(da/dt)$.

[6] Note that ϵ_c does *not* vary during the migration of the secondary, due its mere definition (Table 1).

where

$$\epsilon_{mig} = \epsilon_s - \epsilon_p. \tag{8}$$

Note the mirror-symmetry between the factors ϵ_s and ϵ_p, as expected, the migration of the secondary in one direction has the same effect as the migration of the particle in the opposite direction. Also, the Hamiltonian nature of the motion means that the particle *cannot* be captured in the CER: ϕ_c is either permanently librating or permanently circulating. This has a simple physical interpretation: the particle approaches the corotation radius at the same rate as it recedes from it. This symmetry prevents capture.

However, as ϵ_s is in general *time*-dependent and the particle migration is usually *space*-dependent, capture becomes possible. Here, we make the simplest assumption that the particle migration has a local gradient parametrized by a dimensionless parameter ϵ_g that we define as follows:

$$\frac{1}{n_0 a_0}\frac{da_p}{dt} = \epsilon_p + \epsilon_g\left(\frac{a_p - a_0}{a_0}\right). \tag{9}$$

As we see next, the factors ϵ_s and ϵ_g break the symmetry between the approach to and the recession from CER, possibly leading to capture. In the rest of the paper, all the terms involving the letter ϵ will be assumed to be small compared to unity, corresponding to the fact that the migration rates and their variations are assumed to be small.

3 MIGRATION

The shape of the particle trajectory in the (J_ϕ, ϕ) phase space, in particular the fact that it is in libration or circulation, solely depends on the value of the term into brackets in equation (7):

$$E = \frac{1}{2}\left[\frac{J_\phi}{J_0(t)}\right]^2 - \epsilon_c\cos(\phi_c) + \frac{3}{2}m\epsilon_{mig}(t)\phi_c$$
$$= \frac{1}{2n_0^2}\dot{\phi}_c^2 - \epsilon_c\cos(\phi_c) + \frac{3}{2}m\epsilon_{mig}\phi_c. \tag{10}$$

We have enhanced in the first equation that both J_0 and ϵ_{mig} explicitly depends upon time, due to migration, and we have used $\dot{\phi}_c = n_0(J_\phi/J_0)$ to write the second equation.

The quantity E can be viewed as the dimensionless 'energy' of a particle moving into the 'potential' U of a modified simple pendulum, where

$$U = -\epsilon_c\cos(\phi_c) + \frac{3}{2}m\epsilon_{mig}\phi_c. \tag{11}$$

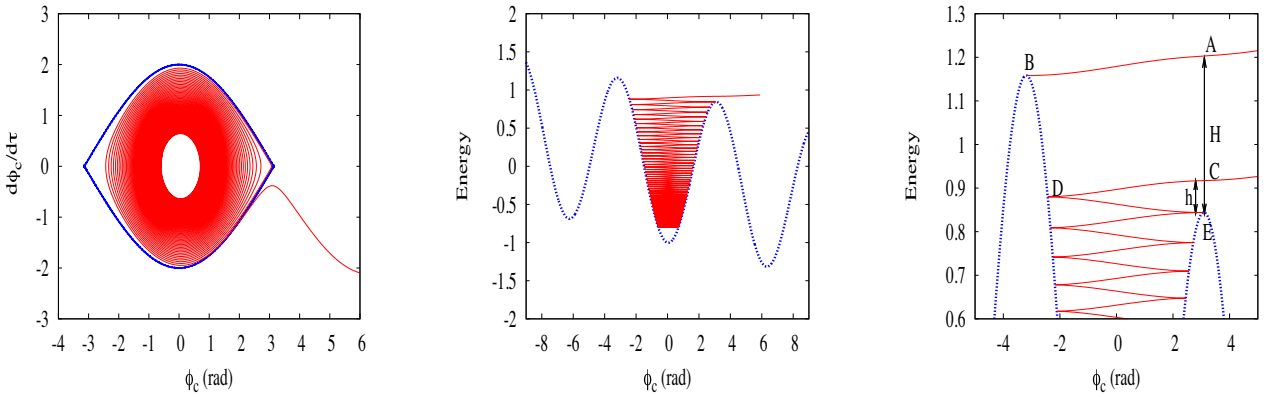

Figure 2. An example of a successful capture in CER, considering a case where $\epsilon_c > 0$. The parameters ($\epsilon_c = 1, \epsilon_{mig} = 5 \times 10^{-2}$ and $d\epsilon_{mig}/d\chi = -5 \times 10^{-3}$) have been greatly exaggerated (compared to practical cases) for better viewing. Note that $\tau = n_0 t$ is a dimensionless time-scale (more details are given in the text). Left-hand panel: phase space (ϕ_c, $\dot{\phi}_c$), where the blue curve represents the separatrix, and the red curve is the captured trajectory illustrated in the right-hand panels. Middle panel (blue curve): the potential energy U (equation 11) versus ϕ_c. Red curve: the total energy E (equation 10). Right-hand panel: vertical expansion of the middle panel, showing the parameters h and H used for the calculation of the probability of capture, see the text.

The function $U(\phi_c)$ is plotted in blue in the two right-hand panels of Fig. 2.

The two slowly varying parameters, J_0 and ϵ_{mig}, together with the term ϵ_g, cause a variation of the energy E:

$$\dot{E} = \frac{dE}{dt} = -\frac{\epsilon n_0}{2}\left(\frac{J_\phi}{J_0}\right)^2 + \frac{3}{2}m\dot{\epsilon}_{mig}\phi_c = -\frac{\epsilon}{2n_0}\dot{\phi}_c^2 + \frac{3}{2}m\dot{\epsilon}_{mig}\phi_c, \quad (12)$$

where $\epsilon = \epsilon_s - 2\epsilon_g$.

A necessary condition of capture is that the particle loses energy E, in order to converge towards a local minimum of U. Ignoring the term in $\dot{\epsilon}_{mig}$ (see the Appendix), this requires

$$\epsilon = \epsilon_s - 2\epsilon_g > 0. \quad (13)$$

A paradoxical result is that ϵ depends on the *migration rate* ϵ_s of the secondary and on the *gradient* ϵ_g of the particle migration rate. In other words, there is a symmetry breaking between the respective effects of the secondary and the particle migrations. This stems from the fact that we consider here the restricted problem.

This effect is described by Sicardy & Dubois (2003), who considered the different, but connected problem of two co-orbital secondary masses m_1 and m_2 suffering slow migrations with rates ϵ_1 and ϵ_2, and gradients G_1' and G_2' (equivalent to the term ϵ_g used here), respectively. Their equation A.13 shows that $\dot{E}$ stems from two terms in front of $\dot{\phi}_c^2$, one proportional to $(m_1\epsilon_1 + m_2\epsilon_2)/(m_1 + m_2)$ and one proportional to $(m_1\epsilon_2 G_2' + m_2\epsilon_1 G_1')/(m_1 + m_2)$. As long as m_1 and m_2 are non-zero, there is a commutativity between the effects of the migrations of the two masses. However, as m_1, say, tends to zero, one obtains a term in ϵ_2 only (equivalent to the term in ϵ_s in equation 13) and a term in $\epsilon_1 G_1'$ only (equivalent to the term in ϵ_g).

Turning back to equation (13), we see that if acting alone ($\epsilon_g = 0$), the secondary migration can lead to capture only if the migration is outwards ($\epsilon_s > 0$). If the particle migration is acting alone ($\epsilon_s = 0$), capture is possible only if its gradient is negative ($\epsilon_g < 0$).[7] In that case, the particle approaches the CER faster than it recedes from it, permitting the capture.

Once the capture is effective, the particle will converge towards a local minimum of U, i.e. the CER centre (Fig. 2). Considering the effect of secondary migration only, one can use an adiabatic invariant argument to estimate how the particle converges to that minimum. Using for instance $\epsilon_c > 0$ and considering a motion close to the stable point $\phi_c = 0$, we have $\cos(\phi_c) \sim 1 - \phi_c^2/2$, and thus, a harmonic motion of the type $J_\phi = J_\phi \cos(\omega t)$ and $\phi_c = \Phi_c \sin(\omega t)$, with $\omega = n_0\sqrt{\epsilon_c}$ and where boldfaces denote amplitudes. The equations $\dot{J}_\phi = -\partial\mathcal{H}/\partial\phi_c$ and $\dot{\phi}_c = +\partial\mathcal{H}/\partial J_\phi$ then provide $J_\phi = \sqrt{\epsilon_c}J_0\Phi_c$, so that the action is $\mathcal{A} = J_\phi \mathbf{\Phi}_c = \sqrt{\epsilon_c}J_0\Phi_c^2$, where $J_0 = \sqrt{GM_c a_0}$. For a slow variation of a_0, $\mathcal{A}$ is adiabatically conserved so that $\sqrt{a_0}\Phi_c^2 =$ constant, thus

$$\Phi_c \propto \frac{1}{a_0^{1/4}}, \quad (14)$$

a result already obtained in the case of co-orbitals bodies by Fleming & Hamilton (2000) and Sicardy & Dubois (2003). Note that the convergence towards the CER centre thus weakly depends upon a_0.

If the particle migration is acting alone, one obtains easily from the previous calculations that $d\Phi_c/dt = (n_0\epsilon_g/2)\Phi_c$, so that

$$\Phi_c \propto \exp(n_0\epsilon_g t/2), \quad (15)$$

where we recall that ϵ_g must be negative for capture to occur. Then the particle converges towards the CER centre on a time-scale $t \sim 2/(n_0|\epsilon_g|)$.

When both the secondary and the particle migrate, the two equations above can be combined to provide

$$\Phi_c \propto \frac{\exp(\int \epsilon_g n_0 dt/2)}{a_0^{1/4}}. \quad (16)$$

Note that the evaluations above can be used to estimate on which time-scales the particle *escapes* the CER libration centre for the cases $\epsilon < 0$. This may happen if the particle is formed inside the CER site, e.g. a dust particle ejected from the surface of a body currently trapped in a CER.

[7] Note that this gradient concerns the *algebraic* value of the migration rate, not its absolute value. For instance an inward migration rate ($\epsilon_p < 0$) whose absolute value decreases with orbital radius will have a positive gradient ($\epsilon_g > 0$).

4 PROBABILITY OF CAPTURE

Fig. 2 illustrates the capture mechanism. It closely follows the path described in Goldreich & Peale (1966) and Murray & Dermott (1999) for capture in spin–orbit resonances. The right-most panel shows that the particle must approach the corotation site through a small energy 'window' h, inside the possible interval H. The particle moves in that plot along the red curve with slope:

$$\frac{\mathrm{d}E}{\mathrm{d}\phi_\mathrm{c}} = \frac{1}{\dot{\phi}_\mathrm{c}}\frac{\mathrm{d}E}{\mathrm{d}t} = -\frac{\epsilon}{2n_0}\dot{\phi}_\mathrm{c}, \tag{17}$$

where we have neglected the term in $\dot{\epsilon}_\mathrm{mig}$ in equation (12), see the Appendix.

The trajectories AB and CDE bound the extreme trajectories that will escape the CER. As those trajectories come very near the hyperbolic points at $\phi_\mathrm{c} \approx \pi$ and $-\pi$, they have energy $E \approx +\epsilon_\mathrm{c}$, so that $\dot{\phi}_\mathrm{c} \approx \pm n_0\sqrt{2|\epsilon_\mathrm{c}|(1+\cos(\phi_\mathrm{c}))} = \pm 2n_0\sqrt{|\epsilon_\mathrm{c}|}\cos(\phi_\mathrm{c}/2)$. Injecting that expression into equation (17), one can integrate $\mathrm{d}E/\mathrm{d}\phi_\mathrm{c}$ to obtain the variations of E along the trajectories AB and CDE. Elementary calculations based on the form of U (equation 11) then provide

$$h = 8\epsilon\sqrt{|\epsilon_\mathrm{c}|} \text{ and } H = 3\pi|m\epsilon_\mathrm{mig}| + 4\epsilon\sqrt{|\epsilon_\mathrm{c}|}, \tag{18}$$

from which the probability of capture $P_\mathrm{m} = h/H$ into the $m+1{:}m$ CER is derived, assuming that the initial energy of the particle is randomly and uniformly distributed in the 'window' H. Substituting the value of ϵ_c as given in equation (2), we obtain

$$P_\mathrm{m} = \frac{h}{H} = \frac{2\epsilon W_\mathrm{CER}}{2\pi a_0|\epsilon_\mathrm{mig}| + \epsilon W_\mathrm{CER}}, \tag{19}$$

where we recall that $\epsilon = \epsilon_\mathrm{s} - 2\epsilon_\mathrm{g}$ and $\epsilon_\mathrm{mig} = \epsilon_\mathrm{s} - \epsilon_\mathrm{p}$. We also recall that the condition $\epsilon > 0$ must be fulfilled for the capture to occur (equation 13).

At this point, we note that in general $W_\mathrm{CER} \ll a_0$, since ϵ_c is very small in equation (2), as $m_\mathrm{s}/M_\mathrm{c}$ and e_s are themselves usually small (Table 1). Moreover, in general, the particle migration rate $\mathrm{d}a_\mathrm{p}/\mathrm{d}t$ does not change rapidly with distance. Taking for instance $\mathrm{d}a_\mathrm{p}/\mathrm{d}t = K/a_\mathrm{p}^q$, where K is a constant and q is usually of order unity, we obtain from equation (9) $\epsilon_\mathrm{g} = -q\epsilon_\mathrm{p}$. As a consequence ϵ_g and ϵ_p are usually of the same order, so that the term in W_CER in the denominator of the equation above can be neglected. Thus, the probability of capture when both the secondary and the particle migrate is

$$P_\mathrm{m} \approx \frac{W_\mathrm{CER}}{\pi a_0}\left|\frac{\epsilon}{\epsilon_\mathrm{mig}}\right| = \frac{W_\mathrm{CER}}{\pi a_0}\left|\frac{\epsilon_\mathrm{s} - 2\epsilon_\mathrm{g}}{\epsilon_\mathrm{s} - \epsilon_\mathrm{p}}\right|. \tag{20}$$

We now examine the two extreme cases where (*i*) only the particle migrates and where (*ii*) only the secondary migrates. In case (*i*), we have $\epsilon_\mathrm{s} = 0$, so that

$$P_\mathrm{m} \approx \frac{2W_\mathrm{CER}}{\pi a_0}\left|\frac{\epsilon_\mathrm{g}}{\epsilon_\mathrm{p}}\right| = \frac{2W_\mathrm{CER}}{\pi a_{\epsilon\mathrm{p}}} \quad \text{(particle migration only)}, \tag{21}$$

where we define $a_{\epsilon\mathrm{p}} = a_0|\epsilon_\mathrm{p}/\epsilon_\mathrm{g}|$ as the radial scale over which the particle migration rate suffers significant changes. We recall here that the condition $\epsilon_\mathrm{g} < 0$ must be fulfilled.

In case (*ii*), we have $\epsilon_\mathrm{p} = \epsilon_\mathrm{g} = 0$ (and $\epsilon_\mathrm{s} > 0$), so that

$$P_\mathrm{m} \approx \frac{W_\mathrm{CER}}{\pi a_0} \text{ (secondary migration only)}, \tag{22}$$

with the noteworthy result that in this case the probability of capture is *independent of the way the secondary migrates*. In other words, we do not need to know the details of that migration to derive the probability of capture. Note also from equation (2) and equation (22) that P_m is *independent of* a_0, since ϵ_c is a constant. In fact, P_m now only depends on ϵ_c and m (i.e. the secondary mass and orbital eccentricity, plus some geometrical factors, see Table 1).

Equation (22) can be re-written by noting that the physical area enclosed in each corotation site (see the physical area enclosed in the blue separatrix in the left-hand panel of Fig. 2) is $4a_0W_\mathrm{CER}/|m|$. Since there are $|m|$ such corotation sites, the total area occupied by the CER is $S_\mathrm{CER} = 4a_0W_\mathrm{CER}$. Moreover, the area enclosed of an orbit of semimajor axis a_0 is $S_0 = \pi a_0^2$, so that

$$P_\mathrm{m} \approx \frac{S_\mathrm{CER}}{4S_0}. \tag{23}$$

Thus, if only the secondary migrates, the probability of capture is one quarter of the area occupied by the CER libration sites divided by the area enclosed in the CER orbit.

5 FULL *N*-BODY SIMULATIONS

We confirm the analytical model described in the previous sections by numerically integrating the full equations of motions. We use the MERCURY integrator package (Chambers, 1999) with the mixed-variable symplectic algorithm, a time-step of 0.02 d, and taking into account the oblateness of the central body up to terms in J_6. We consider the motion of test particles around Saturn and perturbed by the satellite Mimas. The physical parameters of Saturn (mass, radius, oblateness) are given by Cooper et al. (2015), and Mimas ($M_M = 3.75 \times 10^{19}$ kg) is chosen on an equatorial orbit with a semimajor axis $a_M = 185\,536.789$ km and eccentricity $e_M = 0.019\,73$. The migration of the secondary (respectively the test particles) is included by adding a small force to the equations of motion, orthogonal to the radius vector and proportional to the secular migration rate ϵ_s (respectively ϵ_p). We examine various sets of about a hundred test particles migrating outward and crossing $m+1{:}m$ CERs with Mimas, allowing to confirm the analytical formulae for capture probability (Section 4). Initial orbital elements for these particles are chosen randomly, starting from semimajor axis about ten kilometres below the corotation sites. The local gradient ϵ_g is fixed and values for ϵ_p are varied to produce different migration rates (equation 9) and capture probabilities.

Results are presented in Figs 3 and 4. Fig. 3 illustrates the capture process by showing the time evolution of the CER and LER critical angles and of the semimajor axis for a test particle captured into the 3:2 CER. Fig. 4 compares the analytical expression for the capture probability given by equation (21) (particle migration only) with the results of the full N-body integrations, in the case of the 3:2, 4:3 and 5:4 CERs. For these three resonances, the CER and the LER decouple ($D_\mathrm{CL} > W_\mathrm{CER}$). The simulated probabilities are in very good agreement with the analytical estimate given by equation (21). Note that we ensure that the simulated migration rate satisfies an adiabatic criterion in the vicinity of the CER resonance by verifying that the change in semimajor axis produced by the additional force in one CER libration period is much smaller than the CER width.

6 SIMILARITIES WITH SPIN–ORBIT RESONANCES

At this stage, we note that the capture of a particle into a CER resembles the capture of a rotating body into spin–orbit resonance

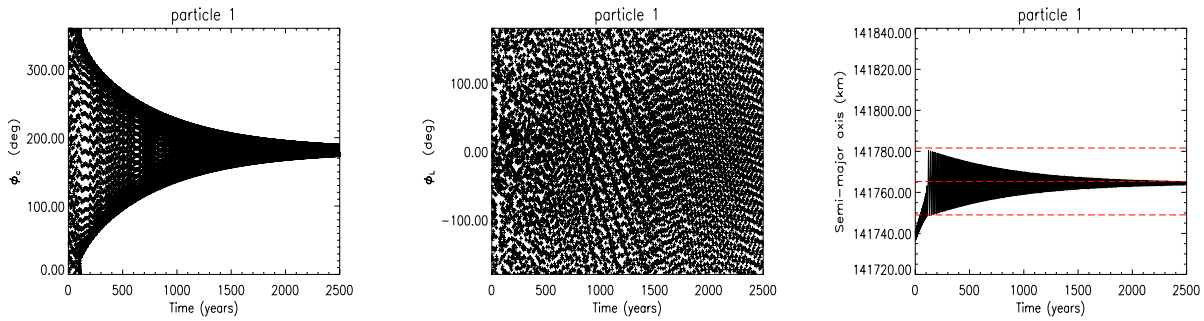

Figure 3. CER, LER arguments and semimajor axis evolution of a test particle, with capture into CER. This example shows the case of the 3:2 CER with Mimas ($e_M = 0.019\,73$) orbiting Saturn on an equatorial orbit. The location ($a_0 = 141\,765$ km) of the CER is indicated by a red dashed line, and the width (32 km) by thinner lines. Note that the radius of the associated LER, $a_L = 141\,897$ km, is outside the semimajor axis range.

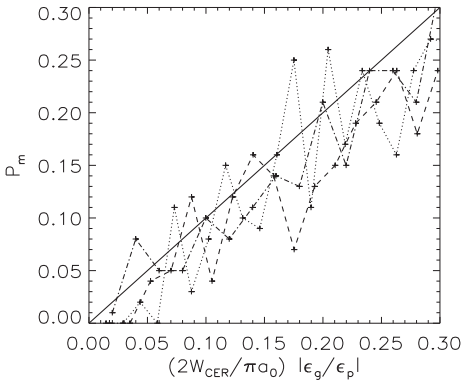

Figure 4. Capture probabilities from full N-body simulations for the 3:2 (dotted), 4:3 (dashed) and 5:4 (dash–dotted) CERs. The solid line is the analytical formula given by equation (21).

(see Goldreich & Peale 1966 or Murray & Dermott 1999). This follows from the fact that the dynamical structures of CERs and spin–orbit resonances are both based on simple pendulum systems. The capture happens because of orbital migration in the case of a CER and tidal friction (and thus migration in the frequency space) for spin–orbit resonances. Using equation (2) and the fact that the libration frequency around the corotation centre is $\omega_0 = n_0\sqrt{|\epsilon_c|}$, one can re-write equation (19) as

$$P_m = N - \frac{4(\omega_0/n_0)}{(3/4)\pi a_0|m||\epsilon_{mig}/\epsilon| + 2(\omega_0/n_0)}. \quad (24)$$

Murray & Dermott (1999) provide the probability of capture into a spin–orbit resonance $\Omega = pn_0$ (where Ω is the spin rate of the body and p is a rational) in two different cases. One of them corresponds to a tidal torque that is dependent on the frequency of each tidal component (the frequency in this context means the one with which the body experiences the tidal distortion), $P_p = 4(\omega_0/n_0)/[\pi V + 2(\omega_0/n_0)]$, see their equation 5.118. The factor V enters in expression of the average, frequency-dependent tidal torque acting on the body $\langle N_s\rangle = -K(V + \dot\gamma/n_0)$, where K is a constant and $\gamma = \theta - pM$ is the spin–orbit resonant angle that relates the body orientation in inertial space, θ, and its mean anomaly, M. By writing the tidal torque $\langle N_s\rangle = N_{s0} + N_{sg}(\dot\gamma/n_0)$, where N_{s0} is the local tidal torque and N_{sg} is its local gradient (in the frequency space), we obtain $V = N_{s0}/N_{sg}$. Therefore, P_p can be written as

$$P_p = \frac{4(\omega_0/n)}{\pi(N_{s0}/N_{sg}) + 2(\omega_0/n)}, \quad (25)$$

identical to equation (24) after posing $N_{s0}/N_{sg} = (3|m|/2)|\epsilon_{mig}/\epsilon|$. In the special case where $\epsilon_s = 0$ (i.e. when only the particle migrates), we obtain $N_{s0}/N_{sg} = (3|m|/4)|\epsilon_p/\epsilon_g|$, which enhances the essential similarities between the CER and spin–orbit captures. Both describe a particle that migrates along the frequency axis of the simple-pendulum phase space at rate N_{s0}, with a local gradient N_{sg} along that axis.

7 DISCUSSION AND CONCLUSIONS

We have studied the mechanism of capture into an isolated first-order CER in the context of the elliptical RTBP, in which a test particle orbits around a central mass M_c, near a first-order mean motion resonance $m + 1{:}m$ with a perturbing secondary of mass m_s. We have derived a formula for the probability of capture given by equation (20) in a general context and performed full numerical simulations (Figs 3 and 4) to confirm its validity.

Then we apply this result to two particular cases, first where we consider a migration of the particle only (equation 21), and secondly, in the case of migration of the secondary (equation 22). We point out the noteworthy fact that in this case, the capture probability does not depend on the way the secondary migrates.

Under realistic assumptions, we have rewritten our formula for capture in the second case as equation (23). This equation has the interesting consequence that if the corotation radius a_0 sweeps a total area S in a region where particles are uniformly distributed with surface density N, then the corotation sites will eventually be populated (due to captures) with a particle surface density of $NS/4S_0$. Conversely, if we observe today a certain number of particles trapped in corotation sites, we may estimate the number of particles originally present in that region.

In particular, our study assumes that the CER is isolated, i.e. that the condition (3) is fulfilled. In the cases where $D_{CL} \sim W_{CER}$, the motion in phase space is chaotic, as the LER and CER are strongly coupled (see Fig. 1). This occurs when the effects of the oblateness of the central body, the presence of a massive disc or another companion in the system, are not strong enough to split and thus isolate the resonances from each other. The chaotic nature of motion then prevents an easy analytical derivation of the probability of capture into the $m + 1{:}m$ mean motion resonance. In that case, numerical integrations might be useful to see whether the probability derived here (equation 19) remains valid, at least in order of magnitude.

This work can be applied in many cases, specially in the context of planetary rings, satellites and exoplanets. As an example, in the context of the Saturn system, El Moutamid et al. (2014) studied the case of Aegaeon that is trapped in a 7:6 CER caused by Mimas, with $a_0 \sim 167\,500$ km. Since $W_{\rm CER} \sim 30$ km, we find a probability of capture of $\sim 5 \times 10^{-5}$. This very low probability suggests that originally, there were many more such objects in the Saturn system, but that only a few of them were captured into CERs. In the context of exoplanets, capture into MMRs in the three-body problem has been investigated in the circular restricted case (one LER only, see e.g. Goldreich & Schlichting 2014) and for systems of two massive planets, ignoring external sources of pericentre precession (Batygin 2015; Deck & Batygin 2015), where the main goal is to explain the rarity of MMR amongst planet pairs and the little statistical preference to be near MMR, as reported by Fabrycky et al. (2014). In the framework of the restricted problem, we are planning in future work to investigate the role of chaos due to the overlap between CER and LER in the escape from MMR.

ACKNOWLEDGEMENTS

The authors are thankful to Philip D. Nicholson, Aurélien Crida, Damya Souami and Matthew M. Hedman for many interesting discussions on this topic. They thank the Encelade working group for interesting discussions and the International Space Science Institute (ISSI) for support. This work was supported by NASA through the Cassini project. Part of the research leading to these results has received funding from the European Research Council under the European Community's H2020 (2014-2020/ERC Grant Agreement no. 669416 'LUCKY STAR').

REFERENCES

Batygin K., 2015, MNRAS, 451, 2589
Borderies N., Goldreich P., 1984, Celest. Mech., 32, 127
Chambers J. E., 1999, MNRAS, 304, 793
Charnoz S. et al., 2011, Icarus, 216, 535
Cooper N. J., Murray C. D., Evans M. W., Beurle K., Jacobson R. A., Porco C. C., 2008, Icarus, 195, 765
Cooper N. J., Renner S., Murray C. D., Evans M. W., 2015, AJ, 149, 18
Crida A., Charnoz S., 2012, Science, 338, 1196
Deck K. M., Batygin K., 2015, AJ, 810, 119
El Moutamid M., Sicardy B., Renner S., 2014, Celest. Mech. Dyn. Astron., 118, 235
Fabrycky D. C. et al., 2014, AJ, 790, 146
Fleming H. J., Hamilton D. P., 2000, Icarus, 148, 479
Foryta D. W., Sicardy B., 1996, Icarus, 123, 129
Goldreich P., Peale S., 1966, AJ, 71, 425
Goldreich P., Schlichting H. E., 2014, AJ, 147, 32
Goldreich P., Tremaine S., Borderies N., 1986, AJ, 92, 490
Hedman M. M., Murray C. D., Cooper N. J., Tiscareno M. S., Beurle K., Evans M. W., Burns J. A., 2009, Icarus, 199, 378
Hedman M. M., Cooper N. J., Murray C. D., Beurle K., Evans M. W., Tiscareno M. S., Burns J. A., 2010, Icarus, 207, 433
Henrard J., 1982, Celest. Mech., 27, 3
Henrard J., Lemaitre A., 1983, Celest. Mech., 30, 197
Murray C. D., Dermott S. F., 1999, Solar System Dynamics.Cambridge Univ. Press, Cambridge
Namouni F., Porco C., 2002, Nature, 417, 45
Nicholson P. D., Mosqueira I., Matthews K., 1995, Icarus, 113, 295
Porco C. C., 1991, Science, 253, 995
Renner S., Sicardy B., Souami D., Carry B., Dumas C., 2014, A&A, 563, A133
Renner S., Cooper N. J., El Moutamid M., Sicardy B., Vienne A., Murray C. D., Saillenfest M., 2016, AJ, 151, 122
Sicardy B., Dubois V., 2003, Celest. Mech. Dyn. Astron., 86, 321
Sicardy B., Roddier F., Roddier C., Perozzi E., Graves J. E., Guyon O., Northcott M. J., 1999, Nature, 400, 731

APPENDIX: EFFECT OF THE VARIATION OF MIGRATION RATE WITH TIME

If the secondary migrates, and since that migration usually depends on the parameter a_0, $\epsilon_{\rm s}$ also depends on time, as well as $\epsilon_{\rm mig} = \epsilon_{\rm s} - \epsilon_{\rm p}$. In that case, the term $(3m/2)\dot{\epsilon}_{\rm mig}\phi_{\rm c} = (3m/2)\dot{\epsilon}_{\rm s}\phi_{\rm c}$ in equation (12) causes a variation of E that should be compared to $-\epsilon\dot{\phi}_{\rm c}^2/2n_0 = -2n_0\epsilon|\epsilon_{\rm c}|\cos^2(\phi_{\rm c}/2)$. In order to simplify the analysis, we assume a simple functional form $\mathrm{d}a_0/\mathrm{d}t = K/a_0^q$, as is done after equation (19). Thus, $\dot{\epsilon}_{\rm s} = -(q-1/2)n_0\epsilon_{\rm s}^2$.

Consequently, in order to neglect $(3m/2)\dot{\epsilon}_{\rm m}\phi_{\rm c}$ with respect to $2n_0\epsilon|\epsilon_{\rm c}|\cos^2(\phi_{\rm c}/2)$, we must have $|m|(q-1/2)(\epsilon_{\rm s}/\epsilon_{\rm c}) \ll 1$. Defining the orbital migration time-scale as $t_{\rm mig} = a_0/\dot{a}_0$, denoting T_0 the orbital period $(2\pi/n_0)$, and using equation (2), the condition above reads

$$\frac{q-1/2}{|m|}\left(\frac{a_0}{W_{\rm CER}}\right)^2 T_0 \ll t_{\rm m}. \tag{A1}$$

Equivalently, this requires that the radial velocity $v_{\rm mig} = \mathrm{d}a_0/\mathrm{d}t$ resulting from the migration of the secondary fulfils the condition:

$$v_{\rm mig} \ll \frac{|m|}{2\pi(q-1/2)}\left(\frac{W_{\rm CER}}{a_0}\right)^2 v_0, \tag{A2}$$

where $v_0 = 2\pi a_0/T_0$ is the orbital velocity.

Those conditions must be checked on a case-by-case basis. For instance, El Moutamid et al. (2014) study the case of Aegaeon which is trapped in a 7:6 CER caused by Mimas, with $m = 6$, $a_0 \sim 167\,500$ km, $W_{\rm CER} \sim 50$ km and $T_0 \sim 0.81$ d. If we consider a Mimas migration caused by tides raised on Saturn, then $q = 11/2$ (Murray & Dermott 1999). The condition (A1) thus requires $t_{\rm m} \gg 20\,000$ yr. This is satisfied by a safe margin, as typical migration time-scales for Mimas are of the order of several millions years (Charnoz et al. 2011; Crida & Charnoz 2012).

This paper has been typeset from a TEX/LATEX file prepared by the author.